# UNDERSTANDING COLD CAP - GLASS MELT CONVERSION FOR WASTE VITRIFICATION AT THE HANFORD SITE, USA

Jessica C. Rigby[1], Anthony M. T. Bell[1] and Paul A. Bingham[1] , Ashutosh Goel[2], John S. McCloy[3], John D. Vienna[4], Kevin M. Fox[5], David K. Peeler[5], Donna P. Guillen[6]

[1]Materials and Engineering Research Institute, Sheffield Hallam University, Howard Street, S1 1WB, UK; [2]Rutgers University, USA; [3]Washington State University, USA; [4]Pacific Northwest National Laboratory, USA [5]Savanah River National Laboratory, USA; [6]Idaho National Laboratory, USA

Sheffield Hallam University | Materials and Engineering Research Institute

U.S. DEPARTMENT OF ENERGY

Pacific Northwest NATIONAL LABORATORY

# The Hanford Site, WA

**65% of total US plutonium production including the Manhattan Project and Cold War**

**200,000m³ of radioactive defence wastes stored in 177 steel tanks**

The Solution:

Vitrification at Hanford's Waste Treatment Plants (WTPs). Final glass wasteform to be stored in geological repositories.

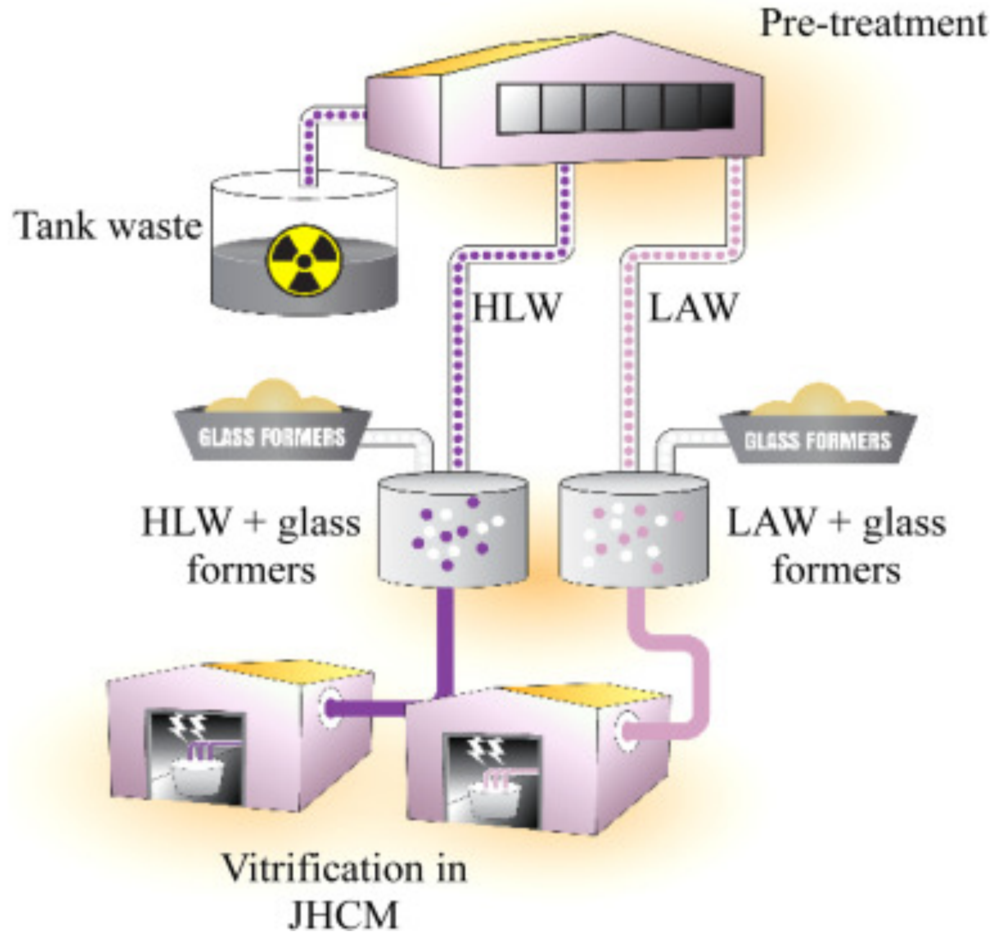

Introduction

Theory

Experimental Methods

HLW-A19

HLW-NG-Fe2

Future Work

# Forming the Cold Cap

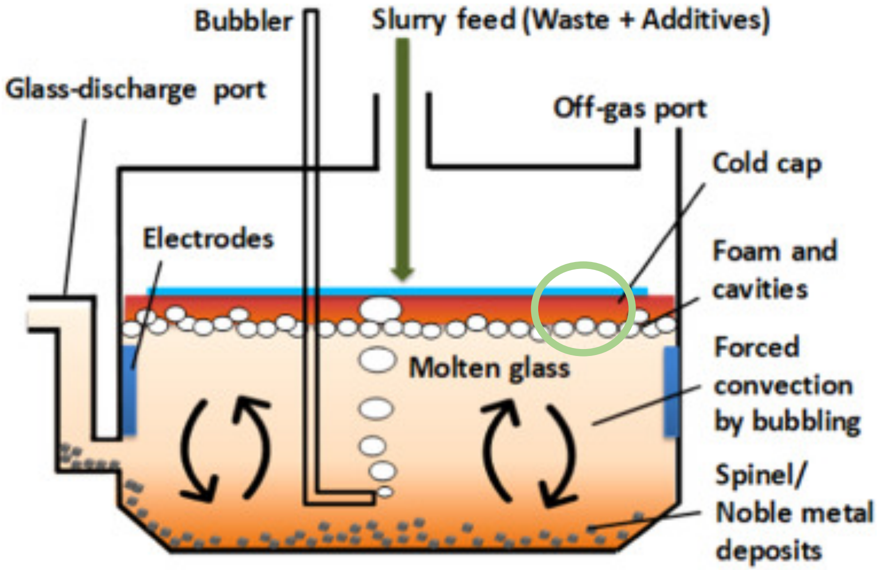


Inside the Joule-Heated Ceramic Melter(P. R. Hrma, Chun, Pierce, & Pokorný, 2013)

- Waste and glass forming chemicals are fed into the top of the melter.
- Electrodes heat the melt to 1150$^{o}$C
- Forced bubbling homogenises the melt
- Glass is discharged through port to cooling canisters
- **Incoming feed creates a batch blanket; the cold cap.**

# Inside the Cold Cap

- Evaporation of Water
- Dehydration
- Decarbonation and denitration
- Low-viscosity melt forming
- Formation of continuous glass forming melt
- *Primary foaming* caused by mostly $CO_2$ evolution
- Primary foam collapse
- Melt viscosity increases
- ***Secondary foaming***
- Dissolution of Quartz
- ***Redox reactions*** and evolution of $SO_2$

*To what extent does the redox state of the melt effect the foaming?*

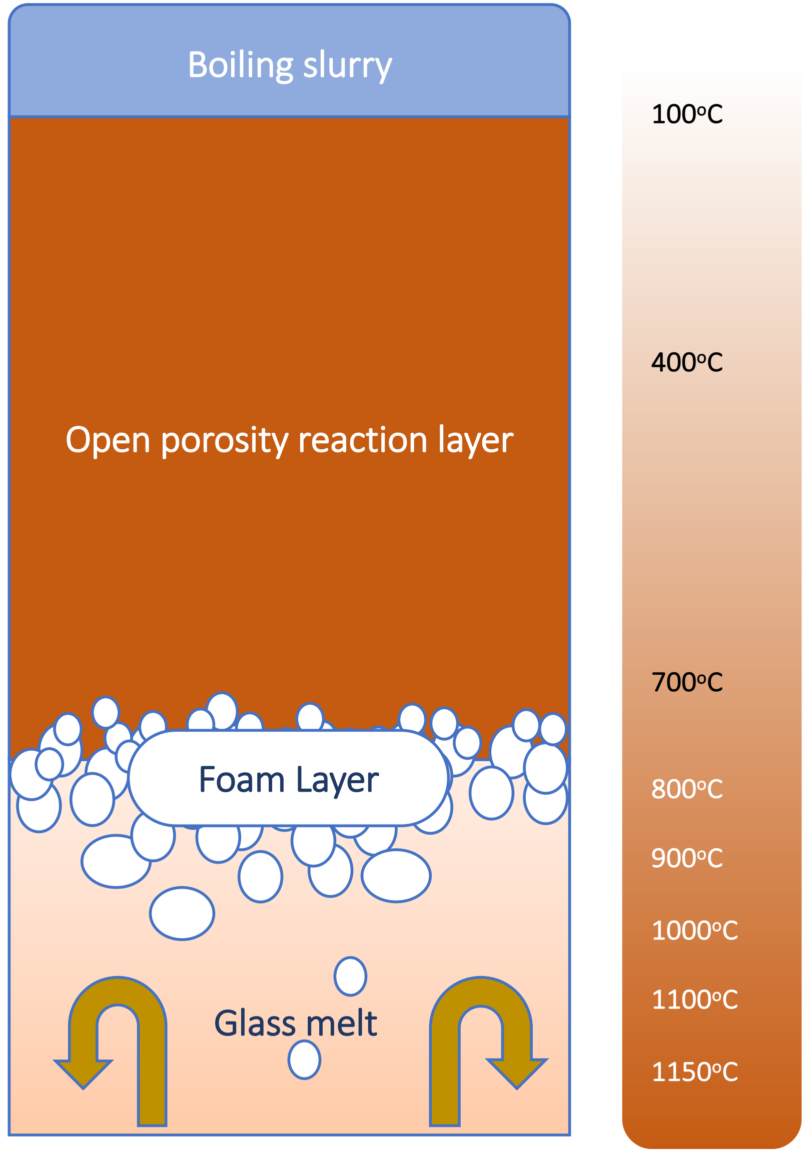


Cold cap profile showing temperature regions. Adapted from (Xu et al., 2016)

Introduction

Theory

Experimental Methods

HLW-A19

HLW-NG-Fe2

Future Work

# Sample Preparation

How can we analyse the cold cap?

- In situ observation
- Mathematical modelling
- Representative samples

## Stages of Melting Study

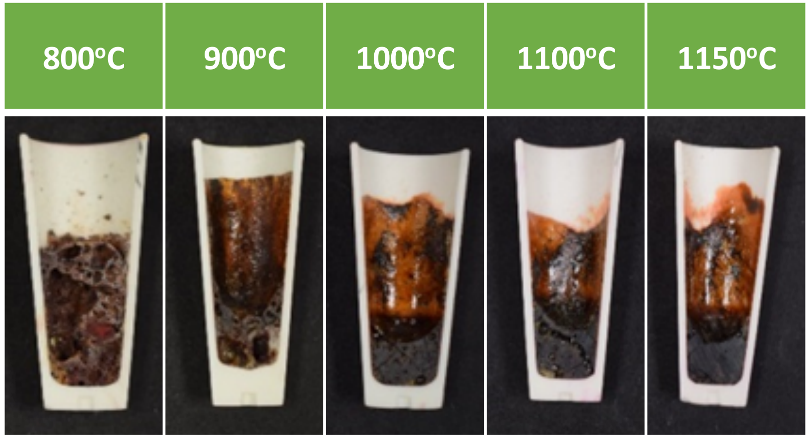


## Feed Expansion Tests


## Laboratory Scale Melter

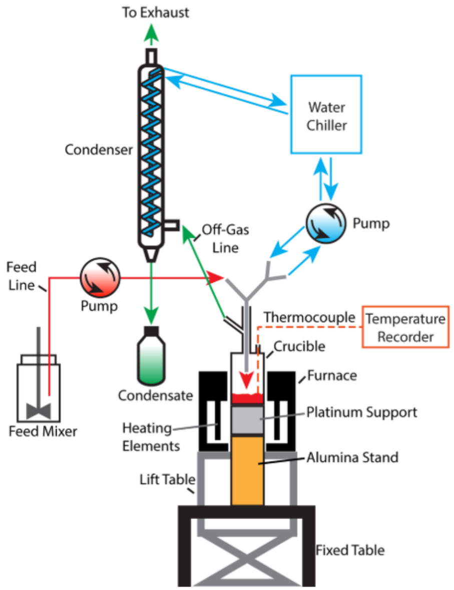


media

Introduction

Theory

Experimental Methods

HLW-A19

HLW-NG-Fe2

Future Work

# Feed Compositions

- Generic, simplified waste compositions
- Specific waste streams with extreme levels of waste oxides:

HLW-A19

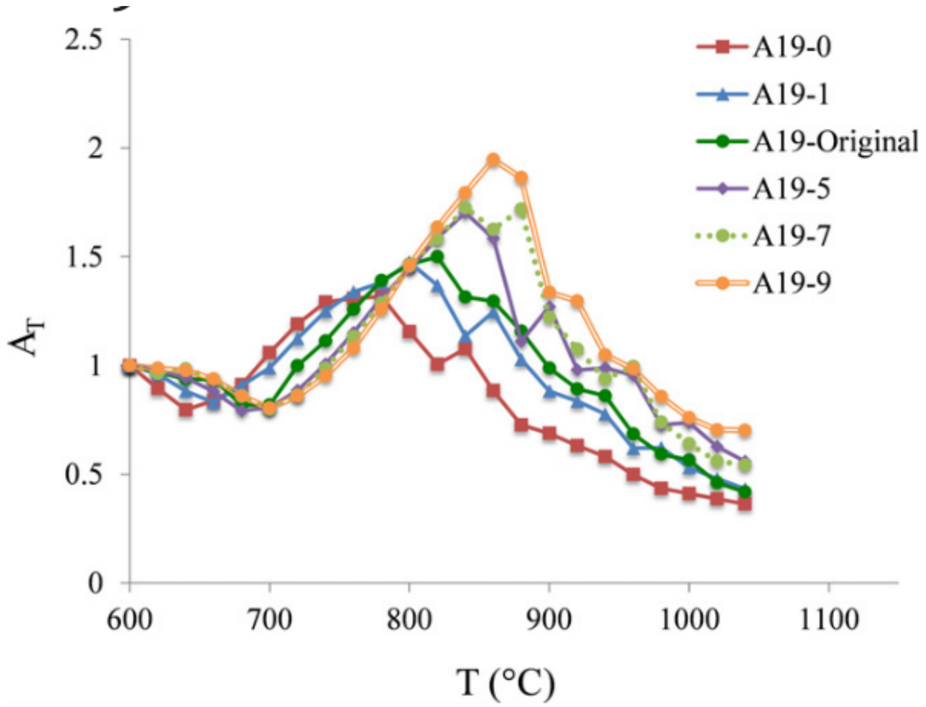


FEED EXPANSION TEST PELLET PROFILE AREA AS A FUNCTION OF TEMPERATURE FOR 6 VARIATIONS OF THE HLW-A19 FEED (HARRIS ET AL., 2017)

| Raw Material | Oxide | HLW-A19/100g | wt% |
|---|---|---|---|
| $Al(OH)_3$ | $Al_2O_3$ | 37.18 | 24.53 |
| $H_3BO_3$ | $B_2O_3$ | 34.16 | 19.41 |
| $CaCO_3$ | CaO | 1.09 | 0.61 |
| $Fe(OH)_3$ | $Fe_2O_3$ | 7.44 | 5.61 |
| $Li_2CO_3$ | $Li_2O$ | 8.92 | 3.64 |
| NaOH | $Na_2O$ | 1.99 | 1.55 |
| $SiO_2$ | $SiO_2$ | 22.15 | 22.35 |
| $Zr(OH)_4.0.65H_2O$ | $ZrO_2$ | 0.55 | 0.40 |
| $Na_2SO_4$ | $Na_2O$ | 0.36 | 0.16 |
| | $SO_3$ | | 0.20 |
| $Bi_2O_3$ | $Bi_2O_3$ | 1.17 | 1.18 |
| $Cr_2O_3.1.5H_2O$ | $Cr_2O_3$ | 0.62 | 0.53 |
| $Ni(OH)_2$ | NiO | 0.50 | 0.41 |
| PbO | PbO | 0.42 | 0.42 |
| $Fe(H_2PO_2)_3$ | $Fe_2O_3$ | 1.25 | 0.40 |
| | $P_2O_5$ | | 1.07 |
| NaF | $Na_2O$ | 1.50 | 0.41 |
| | F | | 0.34 |
| $Na_2CO_3$ | $Na_2O$ | 10.66 | 6.29 |
| $NaNO_2$ | $Na_2O$ | 0.35 | 0.16 |
| $NaNO_3$ | $Na_2O$ | 1.24 | 0.46 |
| $Na_2C_2O_4$ | $Na_2O$ | 0.13 | 0.06 |
| $CaSiO_3$ | CaO | 9.71 | 4.73 |
| | $SiO_2$ | | 5.07 |
| Sum | | 141.366 | 100 |

Introduction

Theory

Experimental Methods

HLW-A19

HLW-NG-Fe2

Future Work

# Feed Compositions

- Generic, simplified waste compositions
- Specific waste streams with extreme levels of waste oxides:

  HLW-A19

  HLW-NG-Fe2

**HLW-NG-Fe2 ($Fe^{3+}$)**

| Raw Material | Oxide | NG-Fe2/100g | wt% |
|---|---|---|---|
| $Fe(OH)_3$ | $Fe_2O_3$ | 20.54 | 15.35 |

**HLW-NG-Fe2 ($Fe^{2+}$)**

| Raw Material | Oxide | NG-Fe2 (II)/100g | wt% |
|---|---|---|---|
| $FeC_2O_4.2H_2O$ | $Fe_2O_3$ | 34.58 | 15.35 |

| Raw Material | Oxide | NG-Fe2/100g | wt% |
|---|---|---|---|
| Al(OH)3 | Al2O3 | 8.61 | 5.63 |
| H3BO3 | B2O3 | 0.56 | 0.32 |
| Na2B4O7.10H2O | B2O3 | 37.16 | 13.57 |
| | Na2O | | 6.04 |
| CaCO3 | CaO | 0.94 | 0.53 |
| CeO2 | CeO2 | 0.12 | 0.12 |
| Cr2O3.1.5H2O | Cr2O3 | 0.30 | 0.25 |
| Fe(OH)3 | Fe2O3 | 20.54 | 15.35 |
| La(OH)3 | La2O3 | 0.11 | 0.09 |
| Li2CO3 | Li2O | 3.87 | 1.57 |
| Mg(OH)2 | MgO | 0.24 | 0.17 |
| MnO2 | MnO2 | 3.98 | 3.98 |
| NaOH | Na2O | 0.81 | 0.63 |
| Na2CO3 | Na2O | 4.04 | 2.36 |
| Ni(OH)2 | NiO | 0.59 | 0.48 |
| FePO4.2H2O | Fe2O3 | 1.71 | 0.88 |
| | P2O5 | | 0.78 |
| PbO | PbO | 0.63 | 0.63 |
| Na2SiO3 | Na2O | 8.03 | 4.08 |
| | SiO2 | | 3.95 |
| Na2SO4 | Na2O | 0.39 | 0.17 |
| | SO3 | | 0.22 |
| SiO2 | SiO2 | 37.33 | 37.33 |
| SrCO3 | SrO | 0.28 | 0.20 |
| ZnO | ZnO | 0.03 | 0.03 |
| Zr(OH)4.0.654H2O | ZrO2 | 1.57 | 1.13 |
| NaNO2 | Na2O | 0.01 | 0.00 |
| NaNO3 | Na2O | 0.45 | 0.16 |
| H2C2O4.2H2O | - | 0.06 | - |
| | | 132.36 | 100.64 |

# HLW-A19 Simplified Stages of Melting Study

| 800ºC | 900ºC | 1000ºC | 1100ºC | 1150ºC |
|---|---|---|---|---|

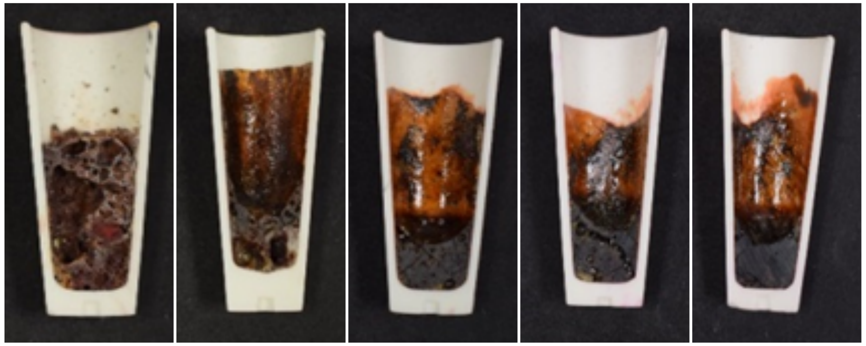

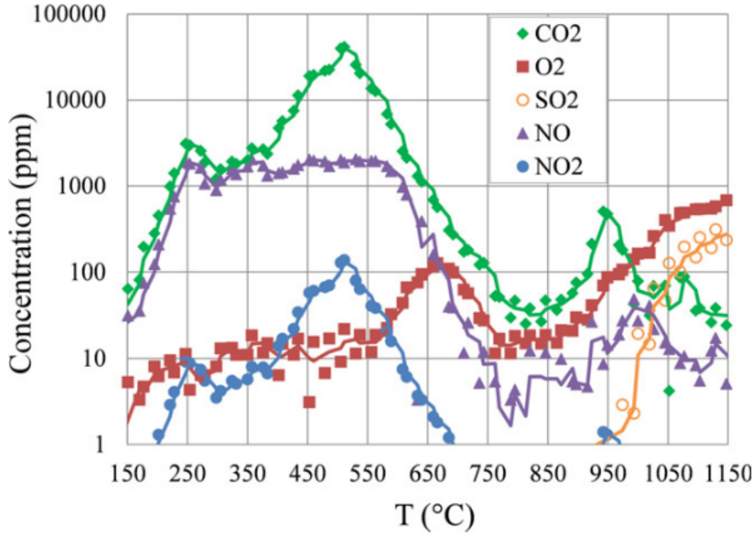


EVOLVED GAS ANALYSIS OF A-19 FEED BETWEEN 150°C AND 1150°C(HARRIS ET AL., 2017)

## Simplified HLW A-19 Composition

| Oxide | Raw Material | mol% | Target wt% | XRF wt% |
|---|---|---|---|---|
| $Al_2O_3$ | $Al(OH)_3$ | 16.73 | 25.13 | 29.16 |
| $B_2O_3$ | $H_3BO_3$ | 19.39 | 19.89 | 19.89 |
| CaO | $CaCO_3$ | 6.63 | 5.48 | 3.20 |
| $Fe_2O_3$ | $Fe_2O_3$ | 3.47 | 8.16 | 10.04 |
| $Li_2O$ | $Li_2CO3$ | 8.47 | 3.73 | 3.73 |
| $Na_2O$ | $Na_2CO_3$ | 10.42 | 9.52 | 7.26 |
| $SiO_2$ | $SiO_2$ | 31.73 | 28.09 | 26.71 |

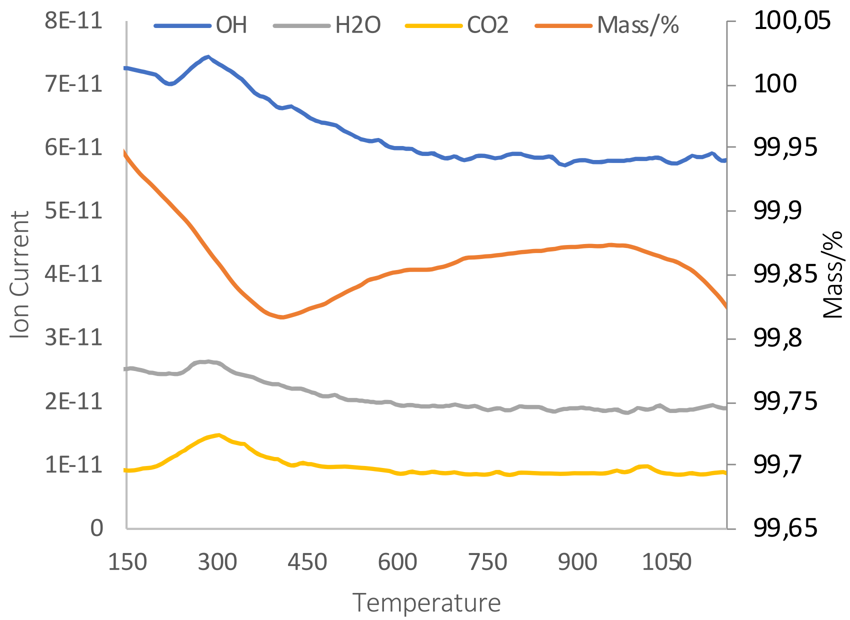


TG-MS OF SIMPLIFIED A-19 BATCH BETWEEN 150°C AND 1150°C

## HLW-A19 LSM Sample

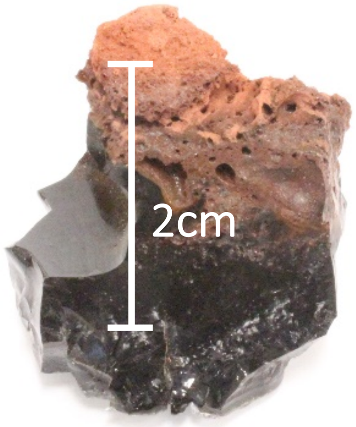


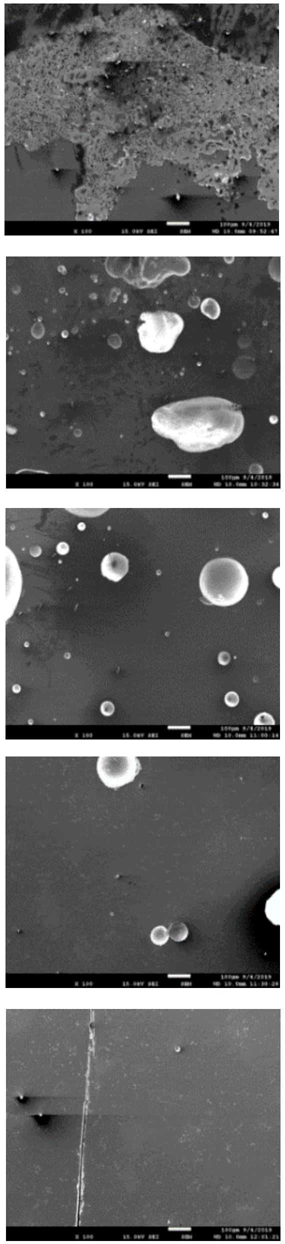

## HLW-A19 Simplified Stages of Melting

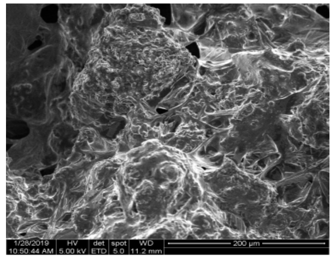

800°C

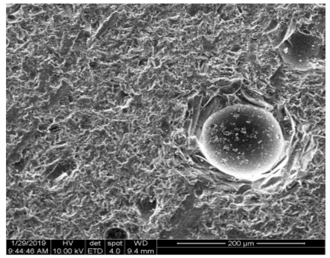

900°C

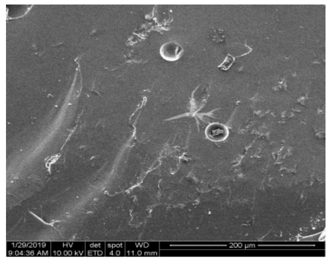

1000°C

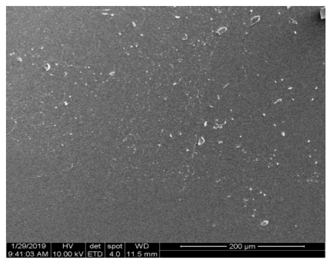

1100°C

Introduction

Theory

Experimental Methods

HLW-A19

HLW-NG-Fe2

Future Work

## HLW-A19 LSM Sample

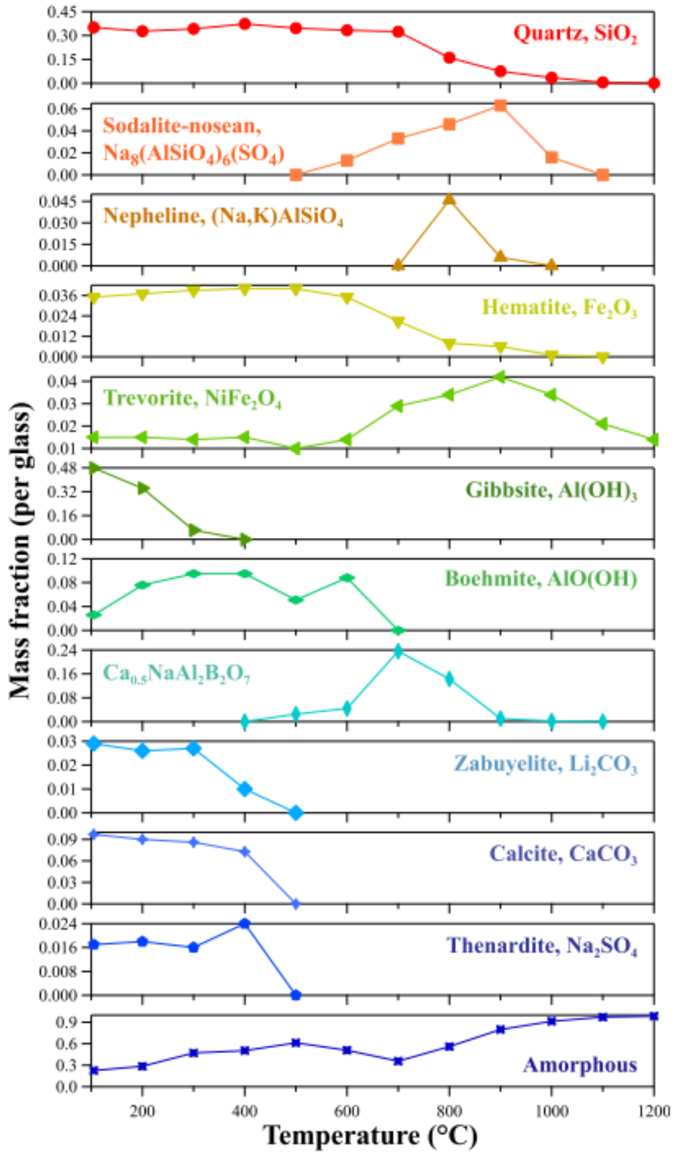


CRYSTAL FRACTIONS IN HLW-A19 STAGES OF MELTING 100°C TO 1200°C (XU ET AL., 2016)

## HLW-A19 Simplified Phase Identification

| | 800°C | 900°C | 1000°C | 1100°C | 1150°C | 1150°C + 1 hour |
|---|---|---|---|---|---|---|
| Quartz | | | | | | |
| Magnetite | | | | | | |
| Hematite | | | | | | |
| Nepheline | | | | | | |

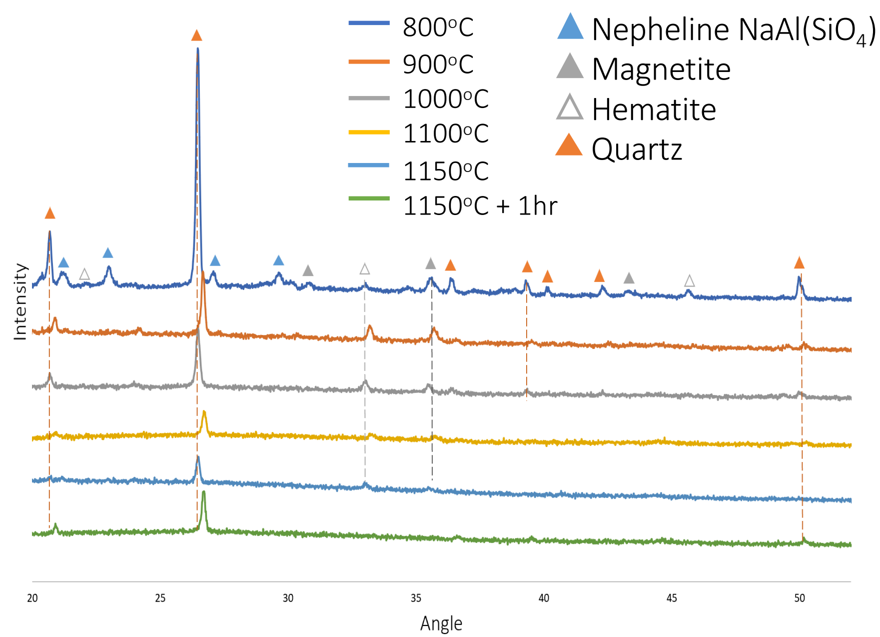

# HLW-A19 LSM Sample EDX

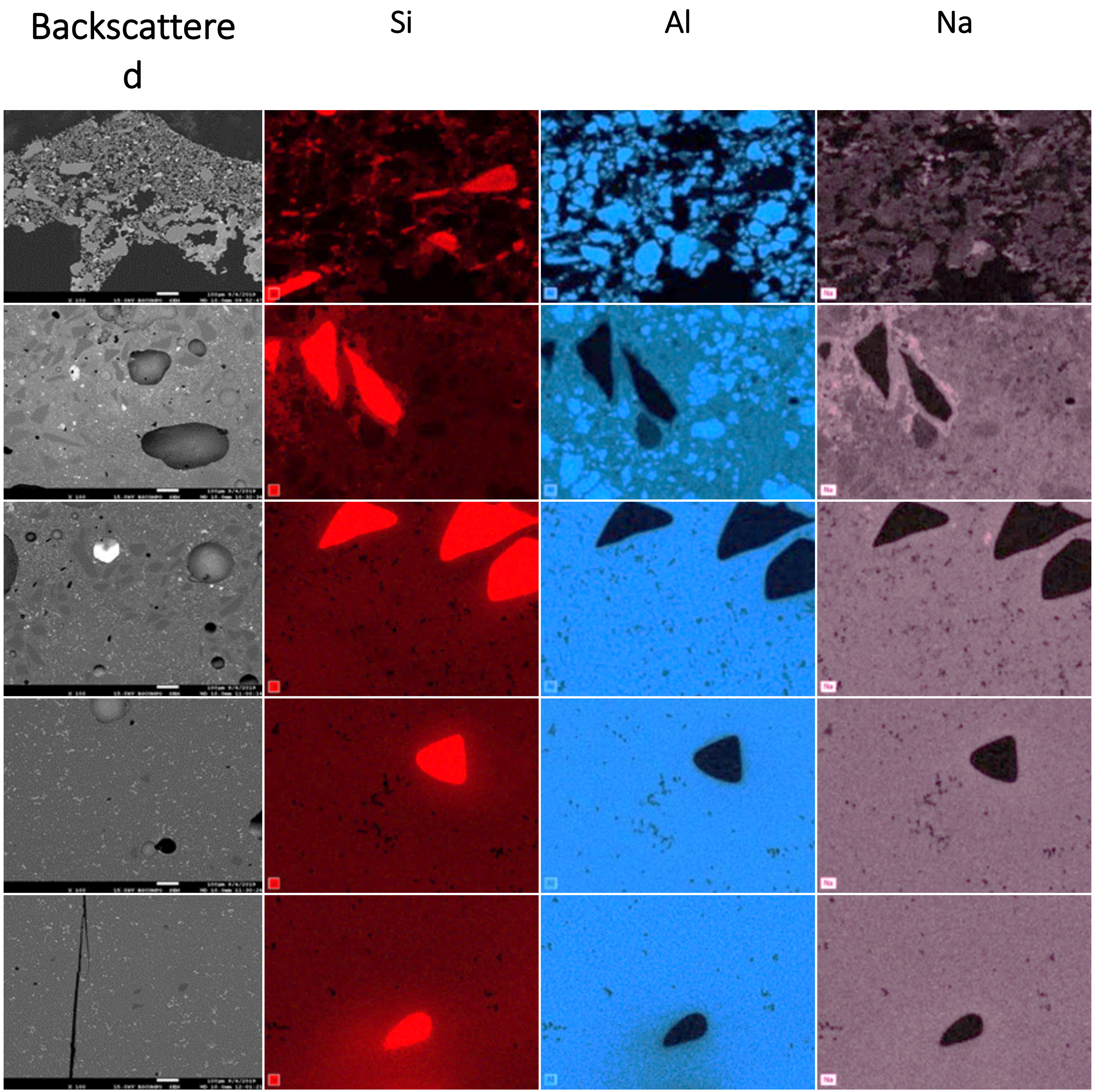

# HLW-A19 LSM Sample EDX

Backscattered | Fe | Ni | Cr

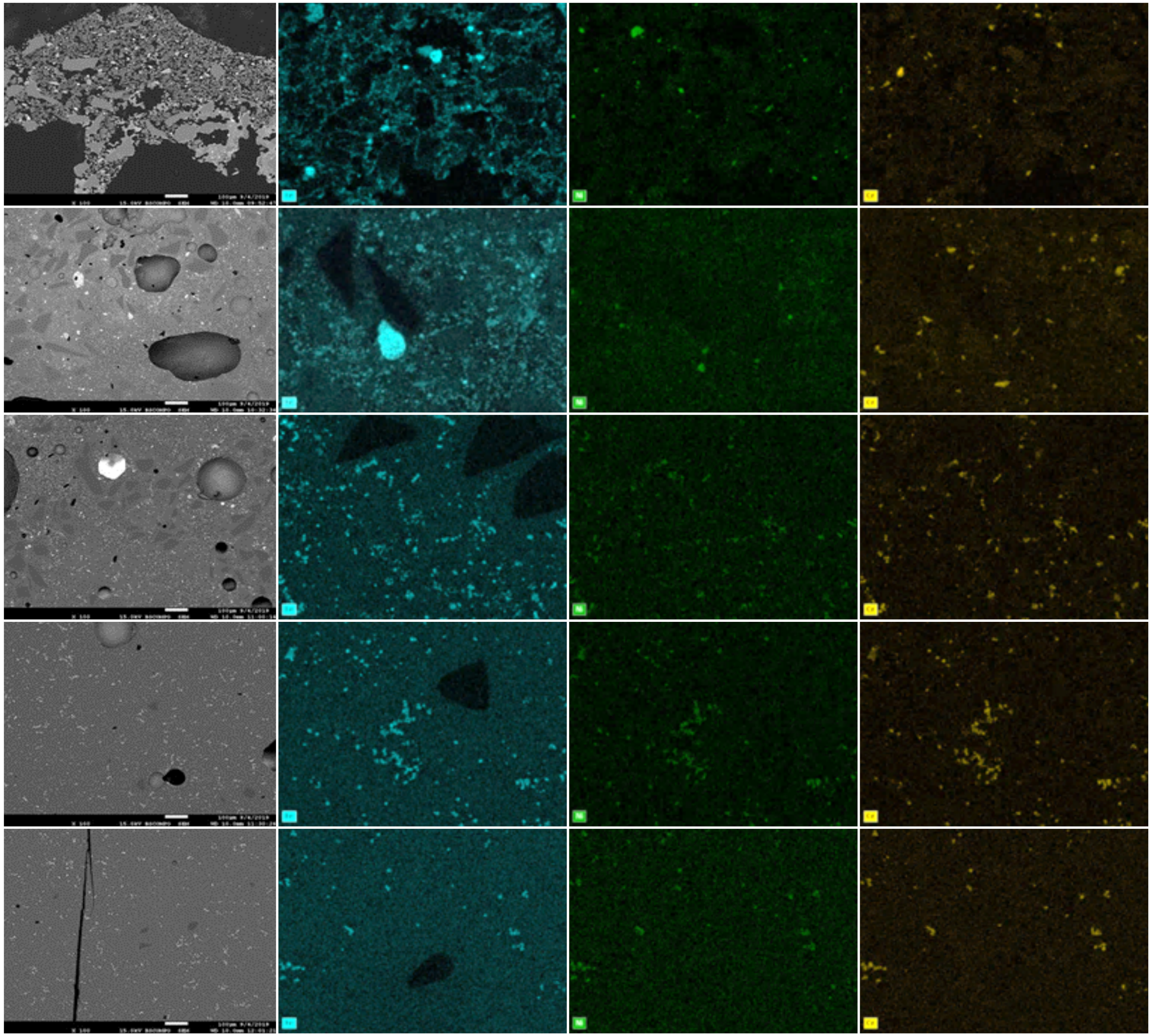

Introduction

Theory

Experimental Methods

HLW-A19

HLW-NG-Fe2

Future Work

# HLW-A19 Discussion

How well did the simplified stages of melting samples represent the cold cap sample?

- Quartz dissolution
- Iron phases
- Gas-evolving reactions
- Phases with other species, e.g. Ni, S, Cr
- Evolution of nitrates and sulphates

Which reactions have been explored in both the simplified and complex feeds?

- Evaporation of Water
- Dehydration
- Decarbonation and denitration
- Low-viscosity melt forming
- Formation of continuous glass forming melt
- Primary foaming caused by mostly $CO_2$ evolution
- Primary foam collapse
- Melt viscosity increases
- *Secondary foaming*
- Dissolution of Quartz
- *Redox reactions and evolution of $SO_2$*

# HLW-NG-Fe2 Fast Dried Slurry Solids

NG-Fe2 $Fe^{3+}$

NG-Fe2 $Fe^{2+}$

# Stages of Melting Samples

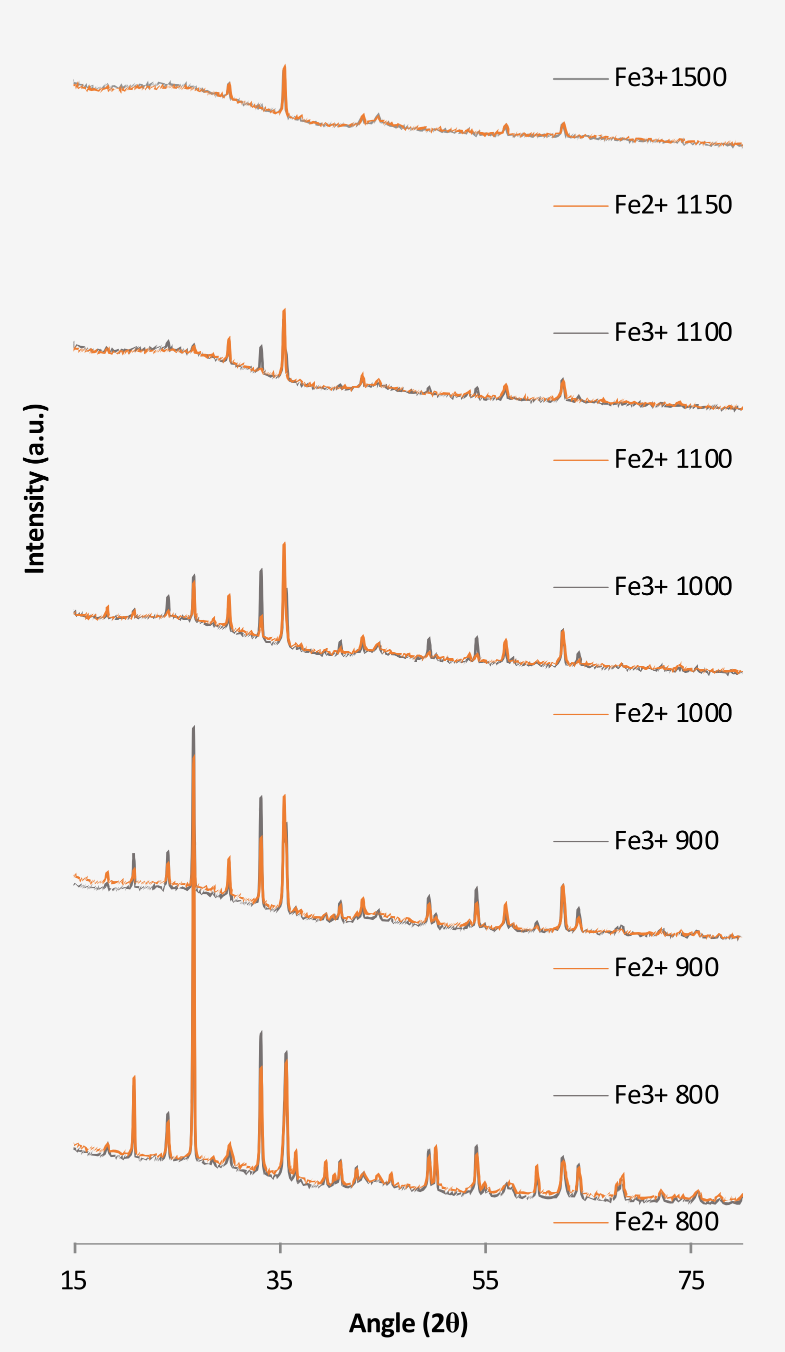


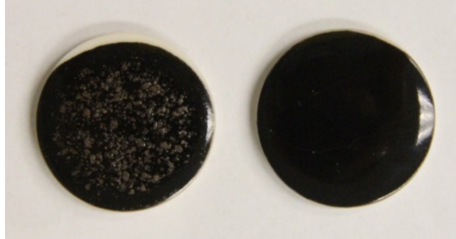

NG-Fe2 $Fe^{3+}$ NG-Fe2 $Fe^{2+}$

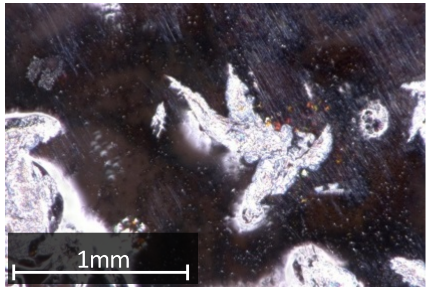


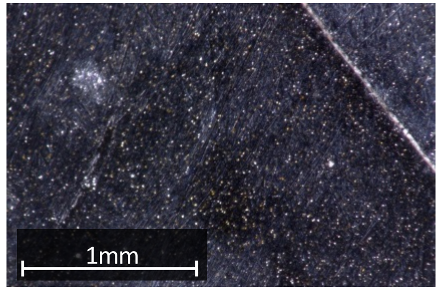


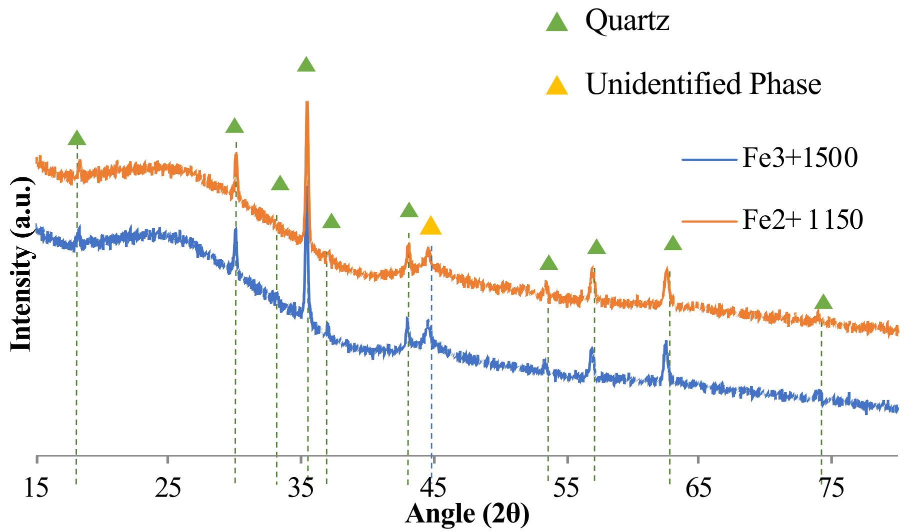

# Feed Expansion Tests

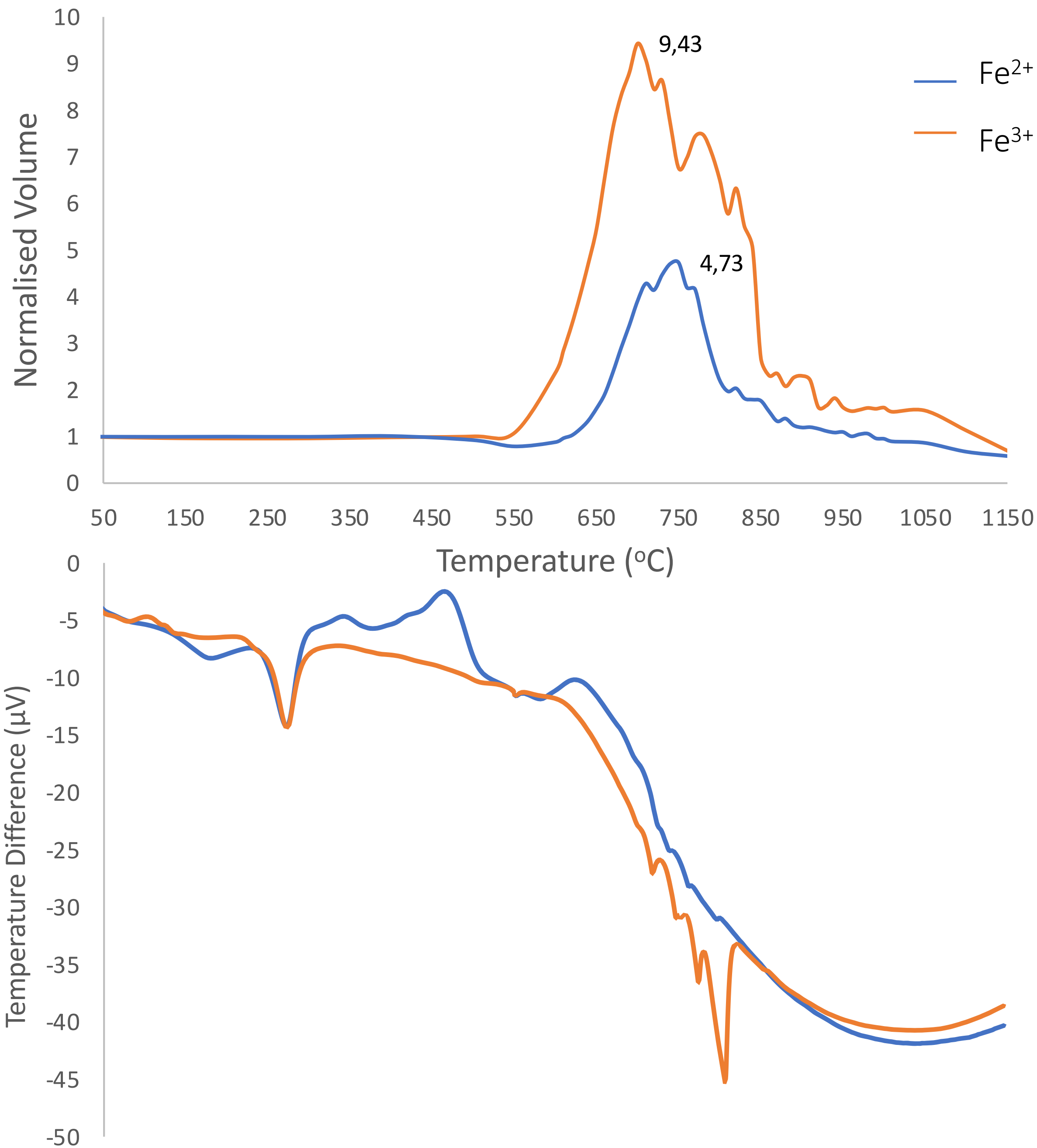


NG-Fe2 $Fe^{3+}$

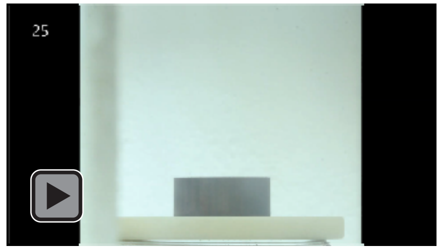


video

NG-Fe2 $Fe^{2+}$

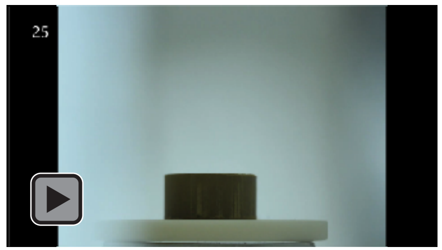


video

# Laboratory Scale Melter

Feed slurry: NG-Fe2 $Fe^{2+}$ (Iron Oxalate)
Feed time: 40 mins
Feed rate: 9rpm

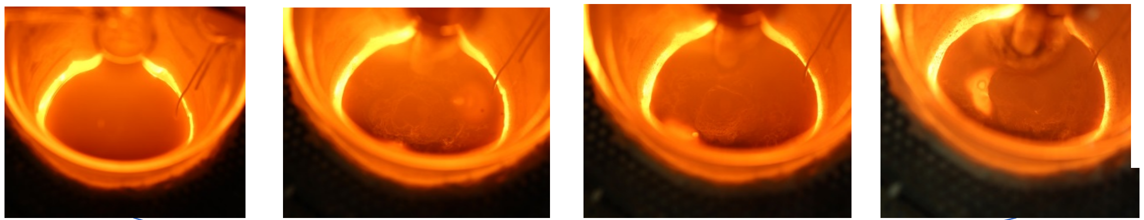

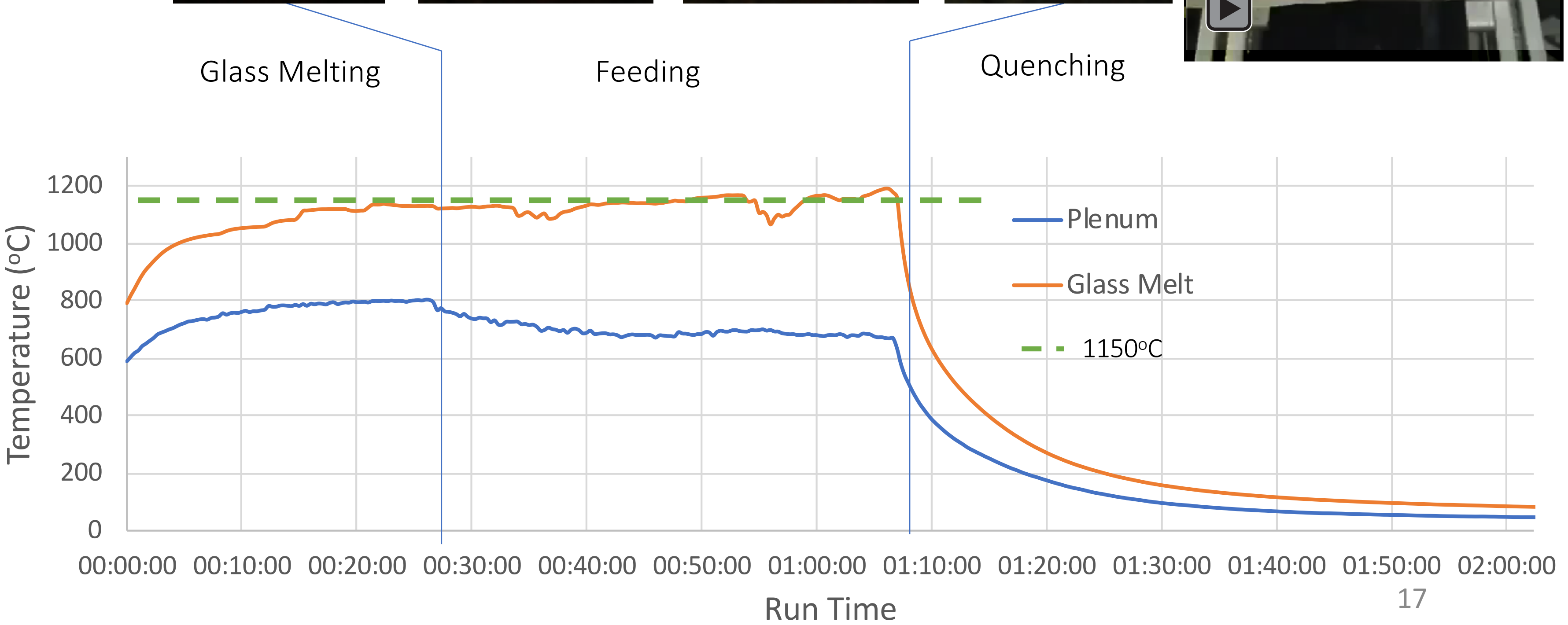

Introduction

Theory

Experimental Methods

HLW-A19

HLW-NG-Fe2

Future Work

# Discussion: HLW-NG-Fe2

| Feed | Raw Material | Fe Oxidation State | Feed/100g | wt% | Normalised Vol. Increase |
|---|---|---|---|---|---|
| NG-Fe2 ($Fe^{3+}$) | $Fe(OH)_3$ | 3+ | 20.54 | 15.35 | 9.43 |
| NG-Fe2 ($Fe^{2+}$) | $FeC_2O_4.2H_2O$ | 2+ | 34.58 | 15.35 | 4.73 |

- Using **Iron Oxalate ($FeC_2O_4.2H_2O$)** in place of **$Fe(OH)_3$** as a raw material for the NG-Fe2 High Iron feed reduces the overall amount of foaming.
- Reduction of foaming may be due to the Fe redox state, but may also be due to the **higher Carbon content**– will be explored further by adding different amounts and sources of carbon as a reductant as well as Mössbauer spectroscopy on the samples.
- Reduced Fe feed was **successful** in the Laboratory Scale Melter, and had reduced feed viscosity.

# Laboratory Scale Melter Sample

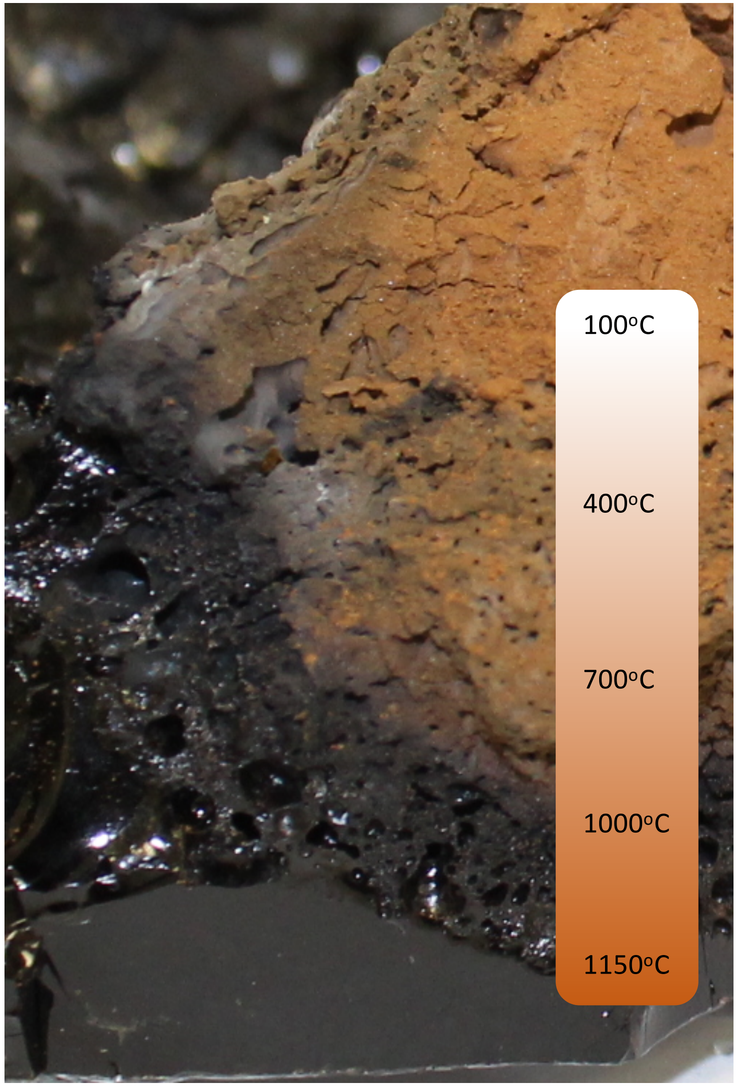


Plan:

- SEM/EDX
- Mossbauer Spectroscopy
- Density/Porosity
- X-ray Absorption Near Edge Structure (XANES)
- Thermogravimetric – Mass Spectrometry

# Future Work

1. Explore effect of altering redox state of raw materials on other feeds high in multivalent species e.g. HLW-E-M09 (High-Cr)

2. Spike simplified compositions with high amounts of multivalent species (Ni, Mn, Cr, etc.) to understand redox effects on a more fundamental scale.

3. Understand the effect of redox reactions on secondary foaming and incorporate this into the wider models for heat transfer in the cold-cap

# Thank you for your attention, any questions?

Sheffield Hallam University | Materials and Engineering Research Institute

U.S. DEPARTMENT OF ENERGY

Pacific Northwest NATIONAL LABORATORY

Paul Bingham
Anthony Bell

Albert Kruger
John Vienna
John McCloy
Kevin Fox
Donna Post Gullien
Richard Pokorný
Ashutosh Goel
David Peeler

Derek Dixon
Derek Cutforth
Jamie George
Pavel Hrma
Seung Min Lee
José Marcial

# References


1. Carles, V., Alphonse, P., Tailhades, P., & Rousset, A. (1999). Study of thermal decomposition of $FeC_2O_4.2H_2O$ under hydrogen. *Thermochimica Acta*, *334*(1–2), 107–113.
2. Dixon, D. R., Schweiger, M. J., Riley, B. J., Pokorný, R., & Hrma, P. R. (2015a). Cold-Cap Temperature Profile Comparison between the Laboratory and Mathematical Model. In *WM 2015 Conference* (pp. 1–9). Phoenix, Arizona.
3. Dixon, D. R., Schweiger, M. J., Riley, B. J., Pokorný, R., & Hrma, P. R. (2015b). Temperature Distribution within a Cold Cap during Nuclear Waste Vitrification. *Environmental Science and Technology*, *49*(14), 8856–8863..
4. Gephart, R. E. (2010). A short history of waste management at the Hanford Site. *Physics and Chemistry of the Earth*, *35*(6–8), 298–306.
5. Guillen, Donna P, & Agarwal, V. (2013). *Incorporating Cold Cap Behavior in a Joule-heated Waste Glass Melter Model INL/EXT-13-29794 Incorporating*. Idaho Falls, Idaho.
6. Harris, W. H., Guillen, D. P., Kloužek, J., Pokorný, R., Yano, T., Lee, S. M., … Hrma, P. R. (2017). X-ray tomography of feed-to-glass transition of simulated borosilicate waste glasses. *Journal of the American Ceramic Society*, *100*(9), 3883–3894.
7. Henager, S. H., Hrma, P., Swearingen, K. J., Schweiger, M. J., Marcial, J., & TeGrotenhuis, N. E. (2011). Conversion of batch to molten glass, I: Volume expansion. *Journal of Non-Crystalline Solids*, *357*(3), 829–835.
8. Hrma, P. R., Chun, J., Pierce, D. A., & Pokorný, R. (2013). Cold-cap reactions in vitrification of nuclear waste glass: Experiments and modeling. *Thermochimica Acta*, *559*, 32–39.
9. Hrma, P. R., & Kruger, A. A. (2008). Nuclear Waste Glasses: Continuous Melting and Bulk Vitrification. *Advanced Materials Research*, *39–40*, 633–640.
10. Hrma, P. R., & Pokorný, R. (2016). *The Office of River Protection Cold Cap and Melt Dynamics Technology Development and Research Plan PNNL-25350*. Richland, WA.
11. Hrma, P. R., Schweiger, M. J., Humrickhouse, C. J., Moody, J. A., Tate, R. M., Rainsdon, T. T., … Tincher, B. H. (2010). Effect of glass-batch makeup on the melting process. *Ceramics - Silikaty*, *54*(3), 193–211.
12. Hujová, M., Pokorný, R., & Kloužek, J. (2018). Vitrification of nuclear waste: Exploring the cold cap. *Sklář a Keramik*, (195), 195–201.
13. Hujová, M., Pokorný, R., Klouzek, J., Dixon, D. R., Cutforth, D. A., Lee, S. M., … Hrma, P. R. (2017). Determination of heat conductivity of waste glass feed and its applicability for modeling the batch-to-glass conversion. *Journal of the American Ceramic Society*, *100*(11), 5096–5106.
14. Joseph, I., Bowan, B. W., Kruger, A. A., Gan, H., Kot, W. K., Matlack, K. S., & Pegg, I. L. (2010). High Aluminum HLW Glasses for Hanford's WTP ORP-42448-FP. In *WM2010 Conference* (pp. 1–13). Phoenix, Arizona.
15. Lee, S., Hrma, P. R., Kloužek, J., Pokorný, R., Hujová, M., Dixon, D. R., … Kruger, A. A. (2017). Balance of oxygen throughout the conversion of a high-level waste melter feed to glass. *Ceramics International*, *43*(16), 13113–13118.
16. Matlack, K. S., Gan, H., Chaudhuri, M., Kot, W. K., Pegg, I. L., Kruger, A. A., … Kot, W. K. (2012). *Melter Throughput Enhancements for High-Iron HLW ORP-54002*. Washington, D. C.
17. Matlack, Keith S, Viragh, C., Kot, W. K., Pegg, I. L., & Joseph, I. (2015). *Effect of the Form of Iron on HLW Melt Rate VSL-15R3430-1*. Washington, D. C.
18. Pierce, D. A., Hrma, P., Marcial, J., Riley, B. J., & Schweiger, M. J. (2012). Effect of alumina source on HLW-feed melting process. *International Journal of Applied Glass Science2*, *3*, 59–68.
19. Pokorný, R., & Hrma, P. R. (2011). *Mathematical Model of Cold Cap — Preliminary One-Dimensional Model Development PNNL-20278*. Richland, WA, USA.
20. Pokorný, R., & Hrma, P. R. (2014). Model for the conversion of nuclear waste melter feed to glass. *Journal of Nuclear Materials*, *445*(1–3), 190–199.
21. Xu, K., Hrma, P. R., Rice, J. A., Riley, B. J., Schweiger, M. J., & Crum, J. V. (2015). Melter Feed Reactions at T ≤ 700°C for Nuclear Waste Vitrification. *Journal of the American Ceramic Society*, *98*(10), 3105–3111.
22. Xu, K., Hrma, P. R., Rice, J. A., Schweiger, M. J., Riley, B. J., Overman, N. R., & Kruger, A. A. (2016). Conversion of Nuclear Waste to Molten Glass: Cold-Cap Reactions in Crucible Tests. *Journal of the American Ceramic Society*, *99*(9), 2964–2970.